

Effect of surface roughness on metal/quenchant interfacial heat transfer and evolution of microstructure

K. Narayan Prabhu ^{*}, Peter Fernandes

Department of Metallurgical and Materials Engineering, National Institute of Technology Karnataka, Surathkal, P.O. Srinivasnagar 575 025, India

Received 24 March 2005; accepted 4 August 2005

Available online 23 September 2005

Abstract

In the present work, the effect of surface roughness on heat transfer rates in various quenchants was determined. The heat flux transients at the probe/quenchant interface were estimated by inverse modeling of heat conduction during end quenching of stainless steel probes with three different surface roughness (grooved, $R_a = 3.0$ and $1 \mu\text{m}$). Heat transfer during quenching was correlated with the hardness obtained for medium carbon AISI 1060 steel specimens. The effect of surface roughness on heat transfer rate during quenching in water and brine was significant for rough surface whereas its effect on heat transfer rate is only marginal in high viscosity oil quenchants. A fully martensitic structure was observed with grooved surface subjected to water quenching. With a smooth surface a mixed microstructure was obtained. The oil quenched specimens were found to be less sensitive to surface roughness.

© 2005 Elsevier Ltd. All rights reserved.

Keywords: Surface roughness; Quenching; Hardness; Steels

1. Introduction

Quenching is one of the most basic and widely used heat treatment processes involving rapid cooling of metal parts from solution treating temperature, typically in the range of 840–870 °C for steel. Quenching is performed to prevent ferrite or pearlite formation and allow bainite or martensite to be formed. Quenching of steel is to harden it and improve its other mechanical properties. This procedure allows the base properties and performances of steels to be significantly enhanced, such that a relatively inexpensive and starting material can be used for a wide range of demanding applications. Heat transfer rate is mainly determined by saturation pressure, thermophysical properties of saturated liquid and by the material, size and shape of the material and roughness of the heating surface. Quenching of steel in liquid medium consists of three distinct stages namely, vapour phase, nucleate boiling, and convective

stage. It is known that in the vapour phase, a vapour blanket is formed immediately upon quenching. This blanket has an insulating effect, and heat transfer in this stage is slow since it is mostly through radiation. As the temperature drops, the vapour blanket becomes unstable and collapses, initiating the nucleating boiling stage. Boiling heat transfer is significantly influenced by the surface condition of the material namely, the purity, oxidation, thickness and roughness of the specimen. Heat removal is fastest in this boiling stage, due to the heat of vapourization, and continues until the surface temperature drops below the boiling point of quenching medium. Further cooling takes place mostly through convection and some conduction [1–3].

The ideal situation is for each stage of the quenching process to occur uniformly on the component to provide uniform transformation with minimum residual stress. Achieving the required hardness, strength or toughness and minimising the possibility of occurrence of quench cracks due to the evolution of residual stresses are the key indicators of a successful hardening process [4,5]. The cooling rates necessary to achieve a desired microstructure mainly depends on the composition, hardenability and

^{*} Corresponding author. Tel.: +91 824 2473756x580; fax: +91 824 2492794.

E-mail address: prabhukn_2002@yahoo.co.in (K.N. Prabhu).

geometry and thickness of the part to be quenched. Cooling rate is depending on the surface rewetting process that occurs for vapourizable quenchants. Expensive, high value-added parts become scrap if insufficient attention is paid to proper quenching. Selection of a quenchant is primarily governed by the processing specifications, the required physical properties, and the required microstructure. Hence, the determination of quench severity and the quantification of the boundary conditions at the metal/quenchant interface would be of considerable utility to the heat treating community. Simulation based quench process design would enable the heat treater to judiciously select the quench medium and prepare the quench surface for a specific application [6,7].

Surface roughness plays a very important role in the transport of heat from metallic surfaces during boiling stage. All boiling regimes are not equally influenced by surface roughness. Sensitivity of boiling regimes to surface geometry during nucleate boiling stage is due to the direct access of the liquid to the surface. Due to an intermittent vapour blanket between liquid and the surface, liquid access is much limited during the transition boiling regime. This results in any surface roughness which is smaller than the thickness of vapour film ineffective at promoting nucleation. This vapour blanket is continuous during film boiling when the effect of surface roughness is less negligible [8].

Drach et al. recognized the presence of active nucleation sites on rough surfaces, which arises by gas entrapment in grooves and cavities [9]. These vapour bubbles pre-exist in relatively large numbers and sizes on rough surfaces and need less superheating to be activated and to initiate nucleate boiling. A series of photographs taken during experimentation to revealed the formation of many small bubbles all over the heated rough surface at the early stages of nucleate boiling. These simultaneously growing bubbles coalesce and form one big bubble, which grows by further vapour generation. The vapour dome grows to a size that is much larger than bubbles which form and detach under stationary conditions. Finally, the large size bubble becomes unstable and is divided into many smaller ascending bubbles.

Luke observed that the large cavities on the rough surface are activated as nucleation sites despite the small superheat or small heat flux at the start of nucleation [10]. Bigger cavities on the rough surface causes higher heat transfer coefficients. More heat transfer is observed with increase in nucleation sites.

Park et al. found that heat the heat transfer rate for rough surface is more than that of smooth surface and is due to the enhancement of wettability in rough surface [11]. The liquid is evenly distributed by providing adequate roughness. A low wettability on the heat transfer surface directly reduced the heat and mass transfer performance. The wettability can be improved by providing surface roughness. Roughness results in a higher wettability by the capillary force on the surface.

Shoji and Zang considered the effect of surface roughness and the temperature on the wettability by measuring

contact angles of water for nucleate boiling system [12]. The surface roughness made the actual area wide.

Wang and Reid considered the effect of wettability of aluminium plates on the effectiveness of an indirect evaporating cooling system. The aluminium plates were coated with about 0.1 mm thickness which gave a lower contact angle compared to the bare aluminium surface leading to a high wettability [13].

Hubner et al. investigated that the enhancement of pool boiling heat transfer at finned tubes with trapezoid shaped fins over a plain tube was mainly due to enhanced bubble formation at the tops of the fins which are very rough [14]. If a uniform surface roughness maintained for finned tube similar to that of plain tube, the enhancement is reduced, resulting in more or less the same heat transfer for plain and finned tube. Heat transfer from finned tubes with special shape (T and Y) of fins considerably improved over a plain tube and trapezoidal shape.

The work carried out so far on heat transfer during quenching is limited to the estimation of estimation of quench severities by various techniques. The effect of surface roughness on heat transfer during quench heat treatment and subsequent evolution of metallurgical microstructure is not yet reported. Hence the present work is aimed at the assessment of metal/quench medium interface for varying surface textures of the metal quenched in aqueous and oil media. The effect of surface roughness on hardness and microstructure is also explored.

2. Experimental work

The experimental set-up consists of a vertical tubular electric resistance furnace open at both ends. A beaker containing 2000 ml of quenchant was placed directly underneath the furnace so that the heated probe could be transferred quickly to the quenching medium. Water, 5% brine, mineral oil and palm oils were selected as the quench media. Quench probes for end quenching were prepared from AISI 304 stainless steel with different surface roughness. Three identical stainless steel probes with 25 mm diameter and 50 mm height with three different surface roughness ($R_a = 1.00, 3.00$ and a groove) at the quench end were prepared. All the probes were instrumented with K-type thermocouples. The thermocouple wires were protected using twin bore ceramic beads. The location of thermocouples and a schematic sketch of the experimental set-up is shown in Fig. 1. The probe was heated to 850 °C in the electric resistance furnace, and was quickly transferred to a beaker containing 2000 ml of the quenchant. The thermocouples were connected by means of compensating cables to a data logger interfaced with the computer.

The following set of experiments were carried out:

1. End quenching of AISI 304 stainless steel probes to study the effect of surface roughness by estimating heat flux transients.

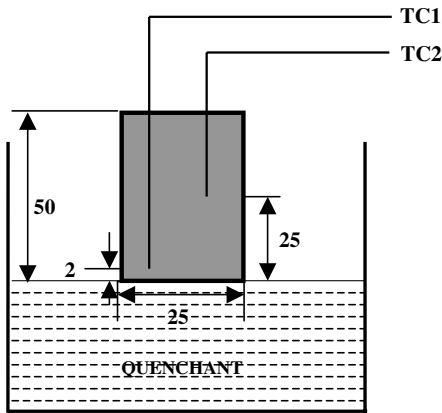


Fig. 1. Schematic sketch of end quenching experimental set-up.

2. End quenching of AISI 1060 steel to assess the effect of surface roughness on hardness.

The composition of AISI 1060 steel used in the present work is given in Table 1.

3. Assessment of heat transfer at the metal/quenchant interface

The non-linear estimation technique of Beck [15,16] has been adopted to analyze the transient heat transfer at the metal/quenchant interface. The one dimensional transient heat conduction equation,

$$\rho C_p \frac{\partial T}{\partial t} = k \left(\frac{\partial^2 T}{\partial x^2} \right), \quad (1)$$

was solved inversely. k , ρ and C_p are the thermal conductivity, density and specific heat of the quench probe, respectively. In this inverse technique, the surface heat flux density is estimated from the knowledge of the measured temperature inside a heat-conducting solid. This is done by minimizing the function,

$$F(q) = \sum_{i=1}^{Ms} (T_{n+1} - Y_{n+i})^2, \quad (2)$$

where $M = \frac{\Delta t}{\Delta \theta}$ (s = a small integer) at regular finite different intervals. T_n and Y_n are the calculated and the measured temperatures at a location close to the metal/quenchant interface, respectively. $\Delta \theta$ and Δt are the time steps for the estimation of heat flux and temperature, respectively. Applying the condition for minimization, the correction for the heat flux (∇q) at each iteration step is estimated. This procedure is continued until the ratio $(\nabla q/q)$ becomes less than 0.005. This procedure simultaneously yields the

Table 1
Composition of the AISI 1060 steel

C	Mn	Si	P	S	Cr	Ni	Mo	Fe
0.58	0.73	0.22	0.042	0.04	0.17	0.048	<0.007	Balance

temperature of the specimen surface in contact with the quench medium and the interfacial heat flux.

4. Results and discussion

Fig. 2 shows the thermal history measured at the two locations (TC1 and TC2) during end quenching of AISI 304 stainless steel probe in 5% brine for smooth (1 μm) and rough surface (grooved) textures. Based on the cooling curves, thermal analysis parameters, namely, peak cooling rate, temperature at which the maximum cooling rate (CR) occurs and the cooling rates at 600, 500 and 400 $^{\circ}\text{C}$ were determined and shown in the Table 2. Cooling rate was found to be strongly dependent on the surface roughness of the probe and the quench medium. Higher cooling rates were obtained for rough surface for water and brine quench media. For example, with brine the cooling rate for rough surface was about 33.33 $^{\circ}\text{C/s}$ compared to the cooling rate of 26.67 $^{\circ}\text{C/s}$ obtained with smooth surface. However an opposing trend was observed for oil quench media. For example, maximum cooling rate of 16.67 and 13.33 $^{\circ}\text{C/s}$ was obtained for smooth surface in palm oil and mineral oil.

The measured temperature history was used as an input to an inverse heat conduction model to estimate the heat flux transients at the metal/quenchant interface. The inverse modeling of heat conduction enables the determination of boundary heat flux transients and the specimen surface temperature. The inverse analysis also yielded the temperature of the probe surface in contact with the quench medium. Estimated heat flux vs. surface temperature plots during end quenching of stainless steel probe with three different surface roughness in 5% brine, water, palm oil and mineral oil are shown in the Figs. 3–6, respectively.

Heat flux transients showed a peak during nucleate boiling stage for all quenchant with different surface roughnesses. The occurrence of peak in the heat flux curve can

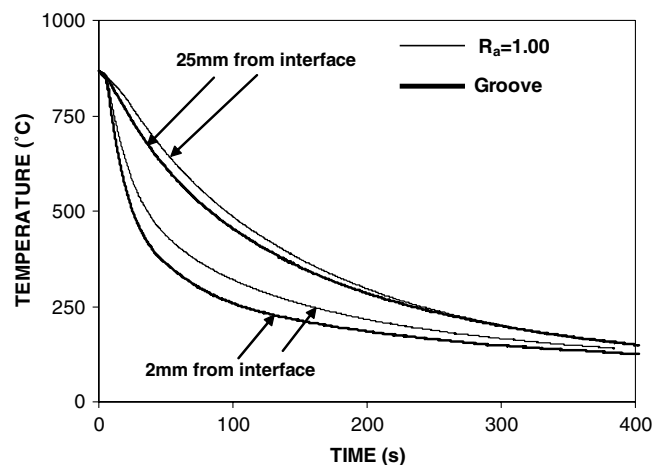


Fig. 2. Cooling curves during end quenching of stainless steel probe in 5% brine.

Table 2
Cooling rate parameters during end quenching of stainless steel probe

Sl. no.	Quenchants	Surface roughness	Peak C.R. (°C/s)	Temp.@max.C.R. (°C)	C.R.@600 °C	C.R.@500 °C	C.R.@400 °C
1	Mineral	$R_a = 1.00$	13.33	645	10.00	10.00	6.67
		$R_a = 3.00$	13.33	635	10.00	10.00	6.67
		Groove	10.00	625	6.67	6.67	6.67
2	Palm	$R_a = 1.00$	16.67	650	13.33	13.33	6.67
		$R_a = 3.00$	16.67	645	13.33	13.33	6.67
		Groove	13.33	635	10.00	10.00	6.67
3	Water	$R_a = 1.00$	23.33	650	16.67	13.33	6.67
		$R_a = 3.00$	26.67	660	20.00	16.67	6.67
		Groove	30.00	675	23.33	20.00	10.00
4	Brine (5%)	$R_a = 1.00$	26.67	665	20.00	16.67	6.67
		$R_a = 3.00$	30.00	675	23.33	20.00	10.00
		Groove	33.33	690	26.67	23.33	13.33

be associated with the peak thermal gradient existing inside the quenched specimen. The water and brine quenchants showed a sharp peak in the heat flux transient curve compared to the oil quenchants as shown in Fig. 7. A maximum peak heat flux of 25.56 kW/m² was obtained with rough surface in 5% brine. The peak heat flux was minimum (10.75 kW/m²) for rough surface texture and mineral oil combination.

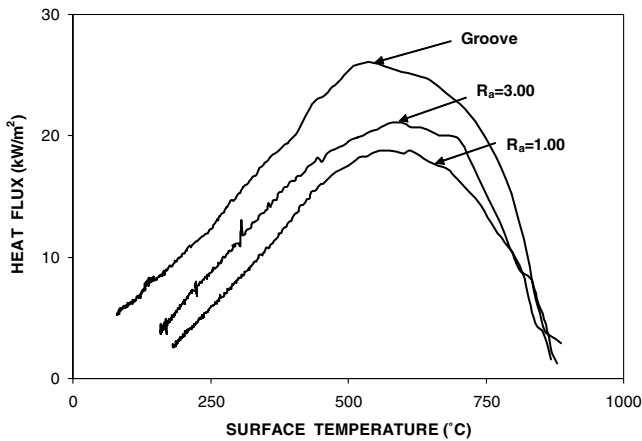


Fig. 3. Heat flux transients vs. surface temperature for quenching in 5% brine.

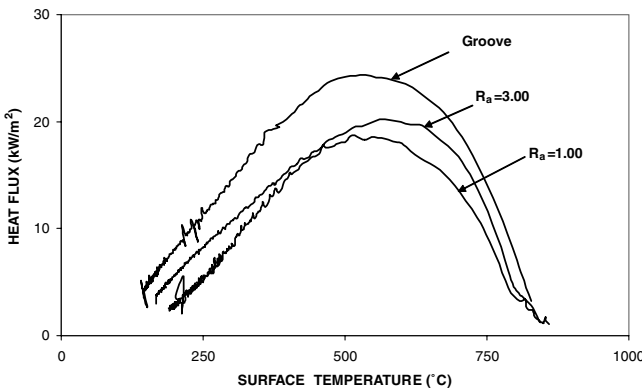


Fig. 4. Heat flux transients vs. surface temperature for quenching in water.

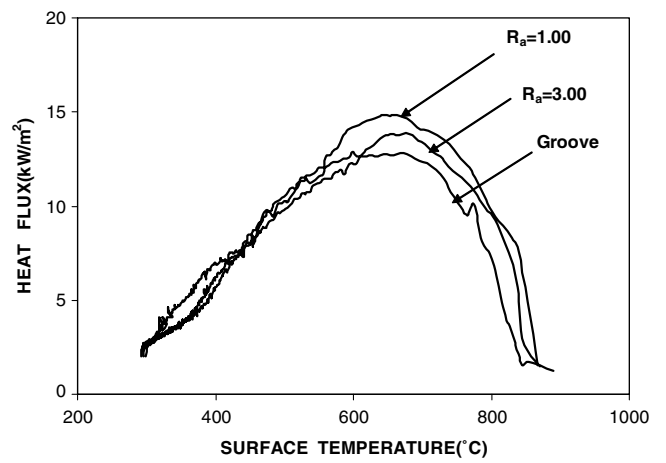


Fig. 5. Heat flux transients vs. surface temperature for quenching in palm oil.

Nucleate boiling stage is slightly delayed in smooth surface compared to rough surface during quenching in water and brine and results in a slight shift in the peak of the heat flux transients towards larger times. This is due to increase in stability of vapour phase in smooth surfaced specimens.

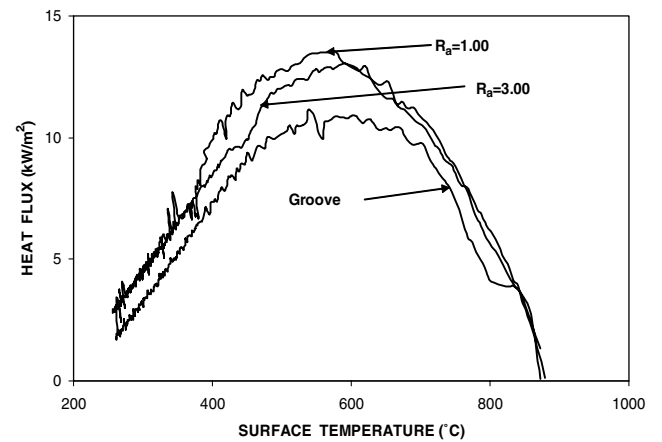


Fig. 6. Heat flux transients vs. surface temperature for quenching in mineral oil.

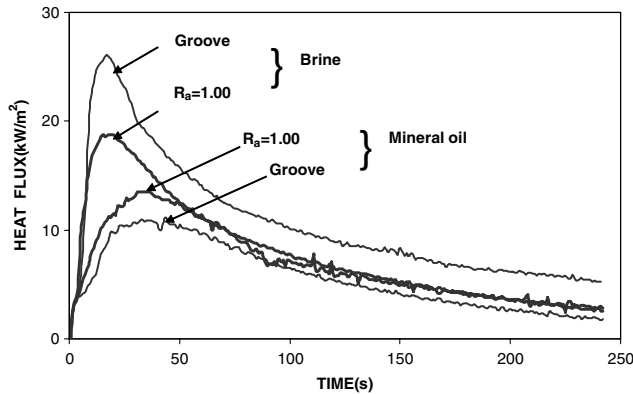


Fig. 7. Effect of surface roughness on estimated heat flux transients during quenching in brine and mineral oil.

However in grooved surface specimens due to sharpness of peaks, the vapour blanket phase collapsed quickly resulting in high rates of heat transfer as shown in Fig. 8. Water and brine quench medium have lower viscosities compared to oil quenchants. The viscosity of water, brine, palm oil and mineral oil at 27 °C are 1, 2, 7.53 and 20.1 mPa s, respectively. Increase in surface roughness of the quench probe is associated with increase in surface area. Water and brine quenchants due to their lower viscosities are able to penetrate easily into the cavities on the rough surface comparing to oil quenchants. The combined effect of lower viscosity and larger surface area available results in significant increase in heat transfer with increase in surface roughness.

Estimated heat transfer coefficients and heat flux transients were lower for rough surface than smooth surface in oil quenchants. This is due to the retention of vapour blanket phase at the valleys of rough surface during nucleate boiling stage though there is boiling at peaks due the large heat transfer. The vapour blanket and boiling stage seem to simultaneously exist resulting in lower heat transfer. Due to retention of the vapour blanket, heat flow rate is reduced which resulted in lower heat transfer coefficients

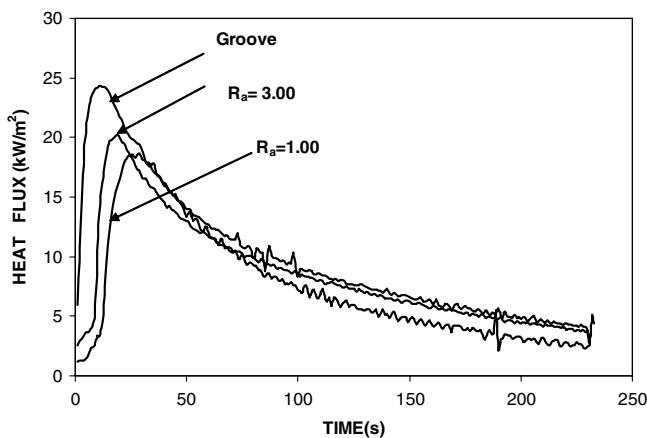


Fig. 8. Effect of surface roughness on estimated heat flux transients during quenching in water.

and heat flux transients. High viscosity of oil is makes it unable to penetrate and wet the surface of valley on rough surface resulting in decreased rate of heat transfer. A schematic sketch of the various stages taking place during quenching with rough and smooth surfaces is shown in Fig. 9(a)–(c). Bubbles of oil adhere to the rough surface in nucleate boiling stage during oil quenching whereas in smooth surface, the bubbles collapsed and move away resulting in higher rate of heat transfer. This continues till the surface temperature at the valley decrease to the boiling temperature of the quenching oil. There is no significant effect of surface texture on heat transfer rate during oil quenching, although increase in surface roughness is associated with increase in surface area.

Fig. 10 shows the hardness profile obtained for AISI 1060 steel specimens with smooth and grooved surface textures subjected to end quenching in mineral oil and water. At 2 cm from the quenched end, the measured hardness was 759 VHN for grooved surface texture with water quench medium. The hardness significantly reduced to 476 VHN at the same location for specimen with a smooth

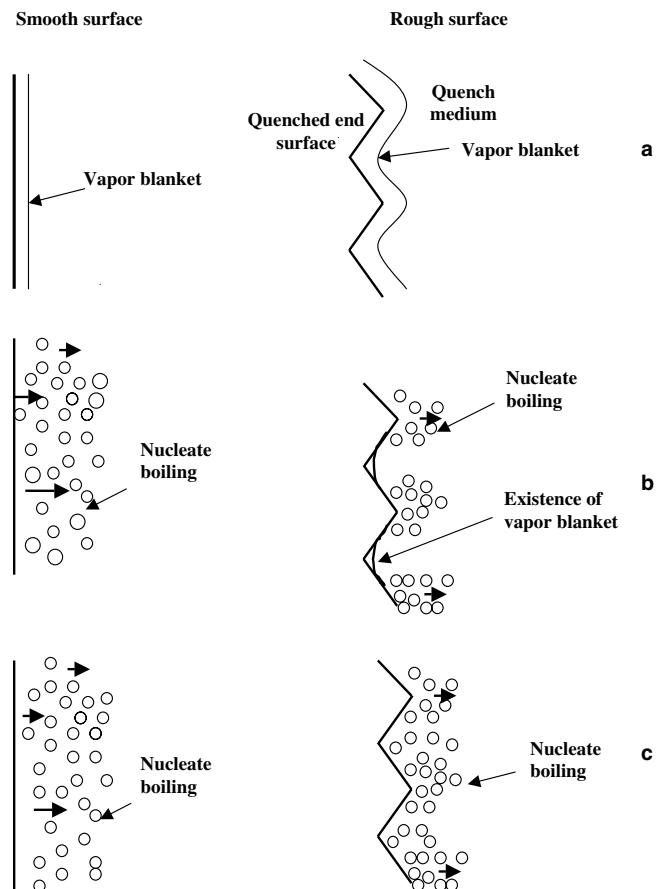


Fig. 9. A schematic sketch to demonstrate the effect of surface texture on vapour phase and nucleate boiling stages during oil quenching: (a) vapour phase stage for both surfaces, (b) nucleating boiling stage for smooth surface and nucleating boiling and vapour phase stage for rough surface and (c) nucleating boiling for both surfaces.

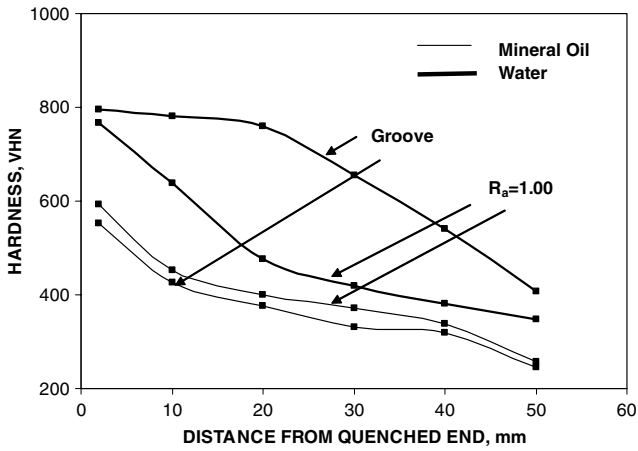


Fig. 10. Hardness vs. distance for specimens quenched in mineral oil and water.

surface texture. For oil an opposing trend was observed with hardness values of 376 VHN and 401 VHN, respectively with rough and smooth surface textures. But the ef-

fect of surface roughness on hardness is less significant in oil quenching. Figs. 11 and 12 show the effect of surface texture on the microstructures of the AISI 1060 steel at 2 cm from the specimen/medium interface for water and oil quench media, respectively. A fully martensitic structure was observed with grooved surface subjected to water quenching. With a smooth surface a mixed microstructure was obtained. The oil quenched specimens were found to be less sensitive to surface roughness. The microstructure consisted mainly of ferrite and pearlite. With rough surface texture, the volume fraction of ferrite phase was slightly larger compared to that obtained for a smooth surface which consisted of significant amount of pearlite.

5. Conclusions

The following conclusions were drawn from the investigation of the effect of surface roughness of the metal on heat transfer and metallurgical microstructure.

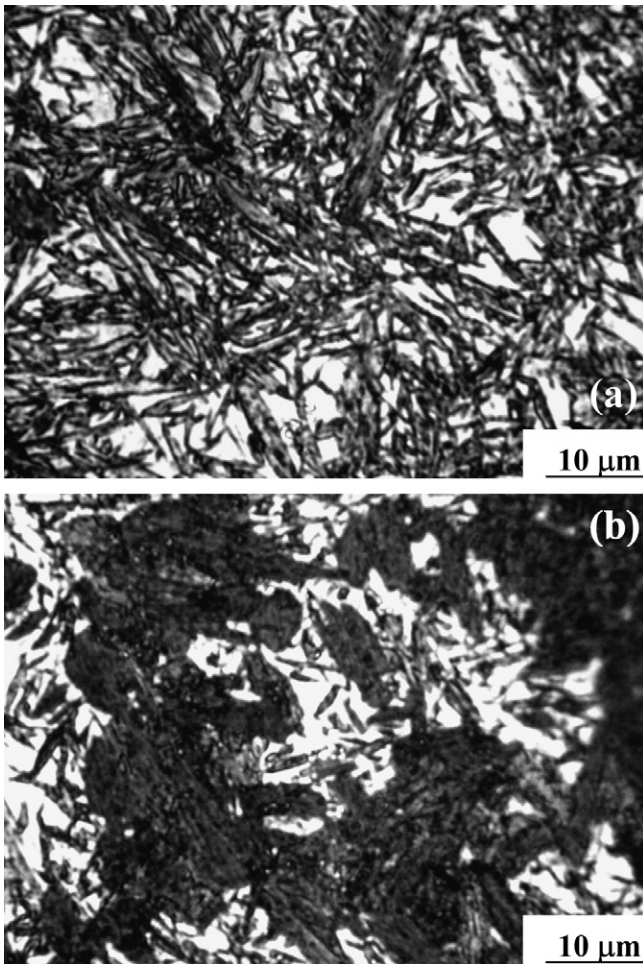


Fig. 11. Microstructures at 2 cm from the specimen/medium interface for water quenched specimens (a) with grooved surface finish showing fully martensitic structure and (b) with smooth surface finish showing mixed microstructure showing mixed microstructure.

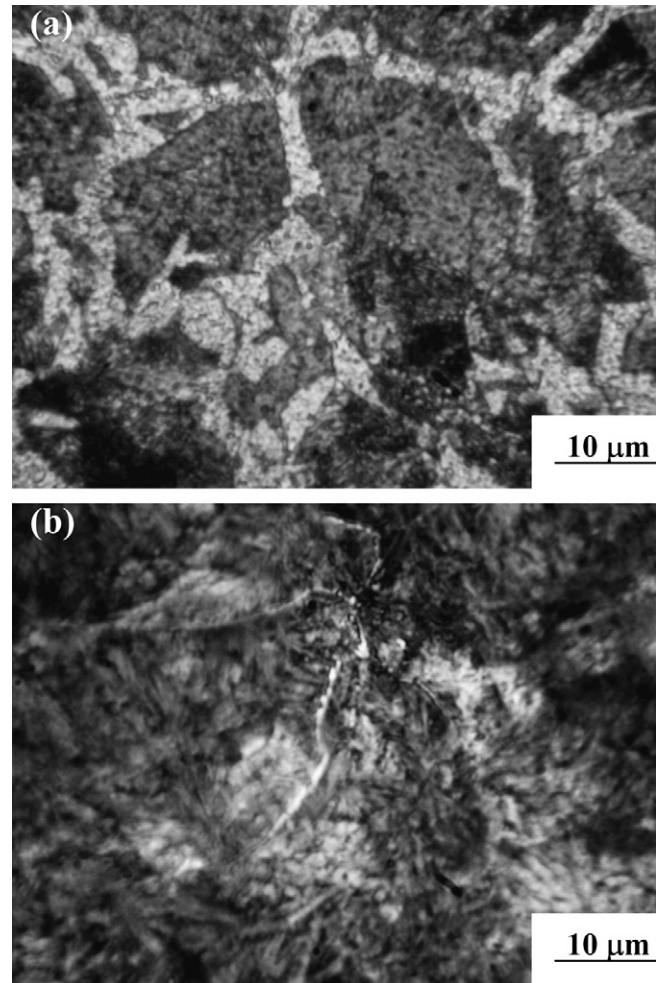


Fig. 12. Microstructures at 2 cm from the specimen/medium interface for oil quenched specimens (a) with grooved surface finish showing ferrite and pearlite (b) with smooth surface finish showing microstructure showing pearlite and ferrite.

1. Heat flux transients estimated using inverse analysis indicated the occurrence of peak heat flux in the nucleate boiling stage for both rough surface and smooth surfaces.
2. The metal/quench medium interfacial heat transfer increased with increase in the surface roughness during quenching in water and brine.
3. An opposing trend was observed for oil quench media with specimens having smooth surface texture yielding higher heat flux transients.
4. For quenching in oils, although the rate of heat transfer is found to be influenced by surface roughness, the effect seems to be less significant compared to that obtained with water and brine.
5. The heat transfer and the hardness data along with the microstructure analysis indicated that the effect of specimen surface roughness on quench heat treatment could not be ignored particularly during quenching in aqueous media.

References

- [1] Metals handbook, 9th ed. In: Heat treating. Materials Park (OH): ASM International; 1981. p. 4.
- [2] Totten GE, Bates CE, Clinton NA. Handbook of quenching and quenching technology. Materials Park (OH): ASM International; 1993.
- [3] Tajima M, Maki T, Katayama K. Study of heat transfer phenomena in quenching of steel. *JSME Int* 1990;33:340–8.
- [4] Van Bergen RT. Effects of quench media selection and control of the distortion of engineered parts. *Mater Sci Forum* 1994;163–165:139–50.
- [5] Totten GE, Sun Y, Webster GM, Jarvis LM, Bates CE. Quenchant selection. In: Proceedings of the 18th Conference of Heat Treating Symposium including the Lui Dai Memorial Symposium. Materials Park (OH): ASM International; 1998. p. 183–9.
- [6] Tszeng C, Nash P. Modeling heat treating processes. *Ind Heat* 2001;68:12–4.
- [7] Tensi HM, Lanier K, Totten GE, Webster GM. Quenching uniformity and surface cooling mechanisms. In: Proceedings of the 16th ASM Heat Treating Society Conference and Exposition. Materials Park (OH): ASM International; 1996. p. 3–8.
- [8] Bernardin JD, Mudawar. Experimental and statistical investigation of change in surface roughness associated with spray quenching of steel. I. *Int J Heat Mass Transfer* 1996;39:2023–7.
- [9] Drach V, Sack N, Fricke J. Transient heat transfer from surfaces of defined roughness into liquid nitrogen. *Heat Mass Transfer* 1996;39:1953–61.
- [10] Luke A. Pool boiling heat transfer from horizontal tubes with different surface roughness. *Int J Refrigerat* 1997;20:561–74.
- [11] Park CW, Cho HC, Kang YT. Effect of heat transfer additive and surface roughness of microscale hatched tubes on absorption performance. *Int J Refrigerat* 2004;27:264–70.
- [12] Shoji M, Zang XY. Study of contact angle hysteresis. *JSME Int J* 1994;37:560–7.
- [13] Wang TA, Reid RL. Surface wettability effect on an indirect evaporative cooling system. *ASHRAE Trans* 1996;102:427–33.
- [14] Hubner P, Wolfgang K. Pool boiling heat transfer at finned tubes – influence of surface roughness and shape of fins. *Int J Refrigerat* 1997;20:575–82.
- [15] Kumar TSP, Prabhu KN. Heat flux transients at the casting/chill interface during solidification of aluminium base alloys. *Metall Trans B* 1991;22:717–27.
- [16] Beck JV. Nonlinear estimation applied to the nonlinear heat conduction problem. *J Heat Transfer* 1970;13:713–6.